ASME Open Journal of Engineering
Online journal at:
https://asmedigitalcollection.asme.org/openengineering

The VD007 Clean-Sheet V12 Diesel Engine: Bridging the Gap Between Diesel Efficiency and Turbine Power in Aviation

Luca Piancastelli
Department of Industrial Engineering (DIN),
Alma Mater Studiorum – University of Bologna,
Bologna 40126, Italy
e-mail: luca.piancastelli@unibo.it

Irene Giusti[1]
Department of Industrial Engineering (DIN),
Alma Mater Studiorum – University of Bologna,
Bologna 40126, Italy
e-mail: irene.giusti4@unibo.it

Marella De Santis
Department of Industrial Engineering (DIN),
Alma Mater Studiorum – University of Bologna,
Bologna 40126, Italy
e-mail: marella.desantis2@unibo.it

Turboshaft and turboprop engines dominate propulsion for light and medium aircraft due to their high power-to-weight ratios and operational reliability. However, their fuel efficiency at partial load remains limited. Compression ignition engines based on common rail diesel technology offer higher thermal efficiency and lower specific fuel consumption, particularly under off-design operating conditions, motivating their investigation for aviation applications in the 300–4000 shp range. This study presents a comparative benchmarking of conventional piston engines and turboshaft propulsion systems to identify efficiency gaps and scaling challenges for aviation diesel engines. The VD007 project investigates a clean-sheet 60-degree V12 Common Rail Diesel Injection Engine (CRDID) architecture featuring dual injectors per cylinder, short-stroke high-speed operation, and a turbocompound configuration for partial exhaust energy recovery. The research combines literature-based benchmarking, structural analyses, and one-dimensional thermodynamic simulations to evaluate the feasibility of the proposed architecture. Experimental validation of the combustion concept was performed on a four-cylinder prototype tested on a dynamometer bench. The experimental campaign produced torque and power curves together with brake-specific fuel consumption values in the range of approximately 163–225 g/kWh. Analytical scaling and system-level simulations of the full V12 configuration indicate a potential output on the order of 2200 HP. The results highlight both the efficiency potential and the current limitations of high-power diesel architectures in aviation, particularly in terms of power-to-weight ratio and system integration. [DOI: 10.1115/1.4071565]

Keywords: diesel propulsion, fixed-wing aircraft, rotary-wing aircraft, high-altitude operation, common rail injection, FADEC control, energy efficiency, engines, mechanical engineering

1 Introduction

Turboprop and turboshaft engines remain the predominant propulsion systems for fixed-wing and rotary-wing aircraft operating below Mach 0.6 or altitudes of 20,000 ft. Their high power-to-weight ratios, operational reliability, and efficient performance across a broad range of flight conditions have established them as the standard choice for general aviation and rotorcraft applications [1]. Despite decades of optimization, recent studies continue to highlight opportunities for improved modeling and performance prediction. For instance, Dursun et al. [2] demonstrated that long short-term memory neural networks outperform conventional artificial neural networks in predicting the thermodynamic and exergetic performance of turboprop engines. Nicolosi et al. [3] investigated advanced turboprop designs for regional missions, identifying configurations capable of reducing fuel consumption and emissions compared to traditional regional aircraft engines.

While modern turbines are increasingly efficient, their performance at partial load remains suboptimal. This limitation, combined with rising operational and environmental costs, has renewed interest in alternative propulsion systems, particularly high-efficiency compression-ignition engines [4]. Among these, common rail diesel injection engines (CRDIDs) have emerged as promising candidates. Ouyang and An [5] highlighted their fuel efficiency, while Xu [6] emphasized their durability. Compared to gasoline engines, CRDIDs reduce fuel consumption by up to 30% at full power and over 50% under cruise or partial-load conditions [7]. Beyond fuel efficiency, diesel engines benefit from simplified internal architectures, enabling longer time between replacement (TBR) intervals, reduced maintenance complexity, and extended component life [8]. Lloyd and Cackette [9] demonstrated that appropriate control strategies, maintenance planning, and fuel adaptation can further reduce emissions without sacrificing operational efficiency. In automotive applications,

[1]Corresponding author.

Manuscript received January 21, 2026; final manuscript received March 26, 2026; published online April 15, 2026. Assoc. Editor: Cosmin E. Dumitrescu.

TBR intervals often exceed 4500 h with only routine oil changes and diagnostics required [10].

Adapting these advantages to aviation could substantially improve dispatch reliability and reduce lifecycle costs. In rotorcraft, where low-altitude and low-speed operation dominate, CRDIDs provide notable fuel efficiency benefits. Moreover, the capability to operate with automotive diesel enhances operational flexibility in austere environments. However, challenges remain: reinforced engine blocks, intercoolers, and turbocharging systems increase weight; reciprocating engines generate higher torsional vibrations than turbines, necessitating improved isolation and drivetrain redesign; and thermal management and combustion control must be optimized for hot-day and high-altitude flight.

1.1 Pathways to Advanced Aviation Diesel Architectures. Research into aviation-grade diesel engines has progressed from automotive conversions to purpose-built architectures optimized for high power. Early work, such as multistage turbocharging on a 1.9 L JTD engine producing nearly 300 HP, illustrated both the potential of advanced boosting and the limits of automotive-derived designs for weight and durability [11]. Two-stroke aviation diesel prototypes have explored twin-turbocharging and electrically assisted boosting to sustain efficiency at high altitudes [12]. Rotorcraft impose additional constraints, including compact vertical packaging, low vibration, and modular gearbox integration. Collectively, these efforts define a pathway from automotive conversions to clean-sheet engines capable of 300–4000 shp in fixed- and rotary-wing platforms.

High-altitude operation introduces additional challenges due to reduced air density, which decreases oxygen availability and alters combustion dynamics. Experiments on a 6.6 L turbocharged common rail diesel showed an 8.7% increase in specific fuel consumption (SFC) and an 8% reduction in thermal efficiency above 3000 m [13]. Modern solutions include variable-geometry and multistage turbocharging to restore sea-level torque at altitudes of 3–5 km [14]. Adaptive injection and boost control are required to maintain ignition timing and in-cylinder pressures [15]. Full authority digital engine control (FADEC) is critical for diesel engines, coordinating injection, turbocharging, and combustion parameters to ensure stable, efficient, and low-emission operation under all conditions [13].

Even with optimized turbocharging, a significant fraction of exhaust energy remains untapped. Turbocompounded hybrid architectures address this by converting exhaust flow into additional shaft power. Historical examples, such as the Napier Nomad, demonstrate the advantages of mechanically decoupled piston-turbine systems for improved energy recovery and flexible load management [16]. Contemporary designs integrate FADEC-controlled coordination to maximize efficiency and endurance in high-performance aviation applications.

1.2 Addressing the High-Power Diesel Design Gap: The VD007 Engine. A comprehensive benchmarking of existing diesel and gasoline engines, presented in Sec. 2, reveals a clear efficiency gap at higher power levels. In smaller power classes, diesel engines demonstrate significant advantages in SFC, often reducing fuel use by 30% at full power and over 50% under partial or regulated load conditions. Despite these benefits, scaling diesel technology to the 1000–5000 shp range presents technical and weight challenges. Adaptations of automotive or high-performance gasoline engines are limited in output and constrained by durability and power-to-weight considerations, leaving a clear design gap for high-power, aviation-grade diesel engines.

The VD007 project was conceived to explore this design gap through a clean-sheet high-power diesel concept. Its architecture features dual combustion chambers per cylinder, each with a dedicated injector, enabling full dual FADEC operation for precise combustion management and improved operational control.

The VD007 concept evolved from earlier experimental work on dual-injector diesel combustion systems developed at the Universitá di Bologna–Alma Mater Studiorum. Experimental validation of the combustion concept was conducted on a dedicated four-cylinder prototype engine tested on a dynamometer bench. These experiments provided preliminary measurements of torque characteristics and brake-specific fuel consumption (BSFC), which serve as a partial validation of the combustion strategy adopted for the VD007 architecture.

The full VD007 engine configuration is based on a short-stroke V12 layout (VD007-II), later refined into the VD007-III configuration incorporating advanced injectors capable of high rotational speeds and improved combustion control. The engine is intended for modular application: turbocharged for helicopters and in a turbocompound configuration for fixed-wing aircraft, potentially combined with a paired turboshaft for redundancy.

In the turbocompound configuration, the VD007 engine recovers a fraction of exhaust energy through a high-pressure turbine mechanically coupled to the compressor and indirectly to the front propeller. Exhaust gases from the diesel cylinders enter the turbine, which drives the compressor stage to boost intake air, thereby enhancing engine efficiency and power output. Simultaneously, the low-pressure turbine of the paired turboshaft converts residual exhaust energy into shaft power that drives the rear propeller in a counterrotating arrangement. This arrangement allows effective power recovery without relying on electrical generation while contributing directly to propulsion and improving overall thermodynamic efficiency.

The mechanical decoupling of the front and rear propellers also provides operational flexibility and fail-safe redundancy. In the event of VD007 failure, the turboshaft can independently maintain rear-propeller thrust, while the system continues to operate safely.

Key specifications include a 12-cylinder V12 layout, a short-stroke configuration, and compact packaging intended for aviation applications. Performance estimates for the complete V12 configuration are derived from analytical scaling and one-dimensional thermodynamic simulations, while experimental validation to date remains limited to the four-cylinder prototype implementing the same combustion concept.

The VD007 project therefore provides a conceptual and analytical framework for investigating high-power aviation diesel architectures. The combination of benchmarking analysis, structural and thermodynamic simulations, and experimental testing of a prototype combustion system offers insight into the feasibility and limitations of scaling diesel technology to aviation propulsion systems.

2 Materials and Methods

This section outlines the methodological framework adopted to evaluate and compare propulsion systems and to develop the VD007 clean-sheet diesel engine. Benchmarking analyses of piston and turboshaft engines were conducted to establish reference baselines in terms of power-to-weight ratio, operating cost, and maintenance philosophy. Cost-per-horsepower-hour metrics were calculated using standardized formulas and industry data, ensuring comparability across engine classes.

To ensure transparency and reproducibility of the cost analysis, the main assumptions used in the cost-per-hour and cost/(hp·h) calculations are summarized here. Fuel costs were estimated using representative aviation fuel prices applicable to the reference year of the analysis. SFC values were taken from manufacturer specifications where available, or from published technical sources for comparable engines. Time between overhaul (TBO) or TBR values were based on manufacturer documentation or publicly available maintenance data. Overhaul reserves were calculated by distributing the estimated overhaul cost over the corresponding TBO/TBR interval. Scheduled maintenance costs were estimated using typical industry maintenance programs, while miscellaneous operating costs were included as a small percentage of the total operating cost to account for auxiliary services and consumables.

The design methodology of the VD007 engine is then detailed, including its architecture, technical specifications, and turbocompound integration strategies. Together, these approaches provide the foundation for assessing the feasibility and performance potential of advanced diesel propulsion in aviation.

2.1 Benchmarking and Critical Comparative Analysis of Propulsion Systems. To contextualize the VD007 engine, a quantitative comparison was conducted across representative piston and turboshaft aircraft propulsion systems. Key metrics considered include rated power, fuel efficiency, maintenance intervals, and operating cost per horsepower-hour.

2.1.1 Selected Engine Characteristics and Operating Costs. Tables 1 and 2 summarize the most relevant piston engine benchmarks. Data are drawn from manufacturer specifications, literature, and the detailed analyses provided in Appendix. VD007 design values are reported for reference.

These data illustrate the efficiency advantage of diesel architectures at higher power levels, with VD007 achieving a low cost per horsepower-hour despite its absolute size and weight.

2.1.2 Sensitivity Analysis. A simple sensitivity study was performed to assess the impact of ±20% variations in fuel price and SFC on operating costs. Variations in fuel price directly shift the total cost per hour, while changes in SFC affect fuel flow and, consequently, cost per horsepower-hour. Engines with inherently low SFC, such as diesel types, retain a relative cost advantage over turboshafts even under realistic fluctuations. This highlights the robustness of the diesel operating cost benefit across plausible market conditions.

2.1.3 Comparison With Turboshaft Engines. High-power turboshafts, such as the Pratt & Whitney PT6A-67D (~1,200 shp) or GE CT7-2E1 (~ 2,000 shp), offer superior power-to-weight ratios but incur substantially higher operating costs (0.45–0.55 USD/(hr·hp)) and complex maintenance requirements. The piston diesel VD007, while heavier per unit power, provides competitive efficiency and lower cost in scenarios where fuel economy and life-cycle cost dominate. Full technical tables, detailed assumptions, and extended cost calculations are provided in Appendix.

2.2 The Gap. In smaller power classes, it has been consistently demonstrated that diesel engines offer significant advantages over gasoline engines, particularly in terms of SFC. At full power, diesel engines typically achieve reductions of approximately 30% in SFC, and under partial or regulated load conditions (off-design), their fuel consumption is often more than 50% lower compared to comparable turboshaft engines. These benefits are largely attributable to the higher thermal efficiency of compression ignition, combined with advances in fuel injection systems, such as high-pressure common rail technology. Given the clear efficiency gap observed in smaller engines, it would be of considerable interest to investigate the feasibility of developing high-power diesel engines—particularly with modern common rail injection—for aviation applications in the 1000–5000 shp class. While technical and weight challenges remain, the potential gains in fuel economy, range, and operational cost could be transformative for certain categories of aircraft. This opens an avenue for research into large-scale, turbocharged or turbocompounded diesel powerplants designed specifically for high-efficiency off-design operation.

A natural first approach to closing this efficiency gap would be to adapt existing high-performance automotive diesel engines for aviation use. However, such conversions are generally limited in output, rarely exceeding ~500 hp, and are constrained by both thermomechanical durability and specific power-to-weight considerations. While feasible for small aircraft or UAVs (unmanned aerial vehicles), this route is insufficient for applications requiring turboshaft-class power levels. An alternative strategy involves converting high-performance gasoline engines—such as those used in sports or racing vehicles—into diesel engines. This has precedent in lower displacement platforms, where manufacturers have transformed spark-ignition engines into common rail diesel engines without the need to redesign entire production lines. Nevertheless, the conversion process is technically demanding. It often entails radical modifications to the original engine block, head, injection system, and thermal management architecture. Moreover, despite such efforts, the resulting power levels tend to remain modest and may not justify the development cost or complexity for large-scale applications. A third, more ambitious pathway is the development of purpose-built high-power diesel engines specifically designed for aviation use. Such engines can be optimized from the outset for high thermal efficiency, off-design performance, and aviation-grade weight constraints. This approach avoids the compromises inherent in adapting automotive platforms and allows for tailored integration of turbocharging, intercooling, and advanced combustion strategies. It is within this context that the "VD007 project" emerges—a clean-sheet initiative aimed at delivering a scalable, high-efficiency diesel powerplant in the ~1000–2000 shp range, with potential modular growth up to ~4000 hp. The project seeks to bridge the existing gap between low-power diesel advantages and high-power aviation demands.

2.3 Methodology and Design of the VD007 Clean-Sheet Diesel Engine. The VD007 Project originated from the observation that most diesel engines derived from the automotive sector exhibit a fundamental limitation in power output, typically around 500 horsepower. These engines are inherently optimized for torque rather than high power, and their fuel systems generally feature a single injector per cylinder, which constrains their potential for performance and redundancy in aviation applications. In response to these limitations, the VD007 engine was conceived around a novel combustion system based on dual combustion chambers and dual injectors per cylinder. This architecture was invented and experimentally validated by Professor Luca Piancastelli at the Università di Bologna—Alma Mater Studiorum, and subsequently patented by the same Institution (see Fig. 1).Table 3 summarizes the main structural and performance parameters of the VD007 V12 diesel engine, providing key values used in the design and analysis presented in this work. It should be noted that the maximum mechanical design speed of the VD007 architecture is approximately 7000 rpm; however, the nominal maximum operating speed considered for performance evaluation and reported in Table 8 is limited to 5000 rpm in

Table 1 Summary of selected piston aircraft engines (technical specs)

Engine model	Power (hp)	Dry weight (kg)	TBO/TBR (h)
Lycoming O-360	180	115	2000
Continental CD-170	170	156	1800
Austro AE300/CD-155	155	185	2400
VD007 (V12)	2143	287	3000–3500

Table 2 Summary of piston engine operating costs

Engine model	Operating cost/h (USD)	Cost/(h·hp) (USD)
Lycoming O-360	92	0.51
Continental CD-170	60	0.36
Austro AE300 / CD-155	61	0.40
VD007 V12	425	0.198

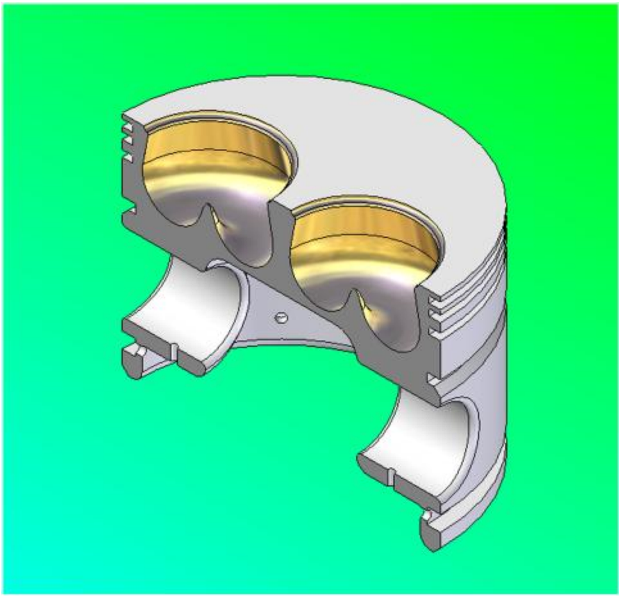

Fig. 1 Cutaway view of the piston featuring dual combustion bowls, each corresponding to one of the two injectors

Table 3 Key structural and performance parameters of the VD007 V12 diesel engine

Parameter	Value
Number of cylinders	12
Bore	142 mm
Stroke	108 mm
Displacement per cylinder	1708 cm^3
Total displacement	20,496 cm^3 (∼20.5 L)
Connecting rod length	180 mm
Crank radius	54 mm
Height	100 mm
Combustion chamber volume	15.8 cm^3
Reciprocating mass per cylinder	7.22 kg
Brake mean effective pressure (BMEP)	2.2 MPa
Maximum peak cylinder pressure	16 MPa
Engine speed at maximum BMEP	3800 rpm
Maximum operating engine speed	5000 rpm
Maximum mechanical design speed	7000 rpm

order to ensure mechanical reliability, thermal stability, and realistic turbocharging conditions. The adoption of two injectors per cylinder is motivated by the need for precise combustion control and high performance across a wide operating range. The dual-injection system enables improved atomization and distribution of fuel within the dual combustion bowls, reducing peak pressure gradients and mitigating the risk of incomplete combustion. Bench testing on the four-cylinder VD007 prototype has confirmed that this architecture produces stable and repeatable combustion, enhances thermal efficiency, and allows optimization of fuel consumption at different engine speeds and loads. These experimental results provide a solid foundation for implementing the same dual-injection strategy in the full V12 engine, ensuring that the system is both feasible and advantageous despite potential reliability concerns.

From a combustion system perspective, the geometry adopted for the VD007 architecture prioritizes structural robustness and compatibility with the dual-injector CRDID concept. The relatively compact combustion chamber diameter and the presence of extended squish regions contribute to promoting mixture motion and mechanical simplicity within the piston bowl configuration.

However, combustion chamber geometries characterized by relatively large squish areas may influence local air–fuel mixing processes and could potentially affect air utilization and soot formation under certain high-load diesel operating conditions. A detailed evaluation of these effects would require dedicated combustion modeling and high-fidelity computational fluid dynamics analyses of the in-cylinder flow field, spray development, and combustion dynamics.

Within the scope of the present work, the combustion system is therefore considered primarily at a conceptual architectural level. The objective of the study is to evaluate the global feasibility of the VD007 engine concept rather than to perform a detailed combustion optimization. Further investigations focusing on spray dynamics, in-cylinder turbulence structures, and emission formation mechanisms are planned as part of future research activities aimed at refining the combustion chamber design.

The design allows for full dual FADEC operation, with a focus on maximizing power output and ensuring reliability for both fixed-wing aircraft and rotorcraft applications. The engine's design is characterized by a short-stroke configuration and initially adopted a V12 layout inspired by the Rolls-Royce Merlin. The configuration later evolved from a V-angle of 90 deg to 60 deg (VD007-II), while maintaining the 12-cylinder arrangement and finally reducing the stroke to accommodate a new generation of ultra-fast injectors (VD007-III). The adoption of dual injectors per cylinder enables the use of state-of-the-art automotive injectors, which are among the most advanced common rail components available due to the scale and investment of the automotive industry. The current iteration of the engine (VD007-III) operates at up to 7000 rpm and delivers approximately 2200 horsepower. Its TBO is set at 500 h, with the target of reaching 4500 h through extended testing and continued development. The VD007 Project has been actively carried forward by students of Professor Piancastelli, to whom the authors wish to express their sincere gratitude. The engine is designed to operate with an absolute intake pressure of approximately 4 bar. In its turbocharged configuration, it is intended for use in helicopters, while a turbocompound version is planned for fixed-wing aircraft, drawing conceptual inspiration from the Napier Nomad engine. An intermediate development stage of the project is represented by the VD007-II, a four-stroke CRDID configured as a 60-deg V12. Designed for high-performance aviation applications, this engine combines high specific power with favorable packaging characteristics. The engine features an 105 mm bore and 120 mm stroke, resulting in a total displacement of approximately 12.45 liters. As shown in Table 4, the total dry mass is 287.35 kg. Table 5 summarizes the key performance characteristics of the VD007 turbocompound system integrated into the Lockheed C-130 powerplant. It presents calculated power outputs for both the 2200 HP VD007 engine and the 867 HP modified PT6 turboshaft, along with combined turbocompound performance, including takeoff and cruise power, engine speeds, and additional thrust contributions. This overview highlights the synergistic interaction between the diesel engine and turboshaft within the aircraft nacelle. Remarkably, despite delivering up to 2200 HP, the VD007-II retains a compact form factor, with an overall length of 1092 mm, a height of 808 mm, and a width

Table 4 Structural mass distribution of the VD007-II V12-60 deg, high-power diesel engine (2000 HP)

Component	Mass (kg)
Accessories	19.5
Crankcase	72.0
Connecting rod assembly	49.6
Gears, mounts, and covers	16.35
Cylinder head and exhaust manifold	110.0
Fasteners	19.1
Total	287.35

Table 5 VD007 turbocompound system integrated in the Lockheed C-130 powerplant, illustrating combined power output and propulsion characteristics

Component	Calculated data
Turboshaft	
Power at takeoff (turbine)	867 HP
Airflow through turbine	3.6 kg/s
Power shaft speed (output)	6000 rpm
VD007 engine	
Maximum power	2200 HP
Engine operating speed	3800 rpm
Maximum rotational speed	5000 rpm
Propellers	
Maximum rotational speed	1450 rpm
Turbocompound engine	
Power (cruise)	3000 HP
Maximum power (takeoff)	3930 HP
Additional thrust (Cruise–Meredith effect)	2620 N

of 750 mm. This dimensional efficiency reflects a design strategy aimed at minimizing engine bay footprint while preserving accessibility and maintainability, as illustrated in Fig. 2, showing the computer-aided design (CAD) model of the VD007-II engine with a 60 deg bank angle, rated at 2200 HP.

The combined power output up to 22,000 ft (6706 m) altitude is 3000 HP, distributed between two countrarotating propellers. The front propeller is driven by the VD007, while the rear propeller is powered by the Pratt & Whitney Canada PT6. In the event of a VD007 failure, the Pratt & Whitney Canada PT6 can independently drive the rear propeller with emergency power, aided by an emergency burner. Under normal operating conditions, air exiting the turboshaft compressor enters the VD007, where it is combusted to produce power for the front propeller. Exhaust gases from the VD007 then drive the high-pressure turbine of the turboshaft, which is mechanically connected to the compressor. The low-pressure turbine of the turboshaft drives the rear propeller. Below the engine, the Meredith duct cools the VD007 while generating additional thrust, optimized for cruise conditions. The Lockheed C-130J Hercules typically cruises at 417 mph (362 knots, Mach 0.59) at an altitude of 22,000 ft (6706 m). The engine nacelle has dimensions similar to the original Lockheed C-130J design. The total mass of the propulsion system is about 750 kg. Figure 3 presents a detailed CAD view of the VD007-II crankshaft, with a focused zoom highlighting its configuration on the bearing support and the geometric relationships between journals, bearings, and main supports. In contrast, Fig. 4 depicts the complete VD007 turbocompound engine assembly, showing the 3930 HP VD007 coupled with a modified 867 HP Pratt & Whitney Canada PT6 turboshaft, fully installed within the engine nacelle of a Lockheed C-130J. This figure illustrates the entire CAD model, including all major components, connections, and the integration layout within the aircraft structure.

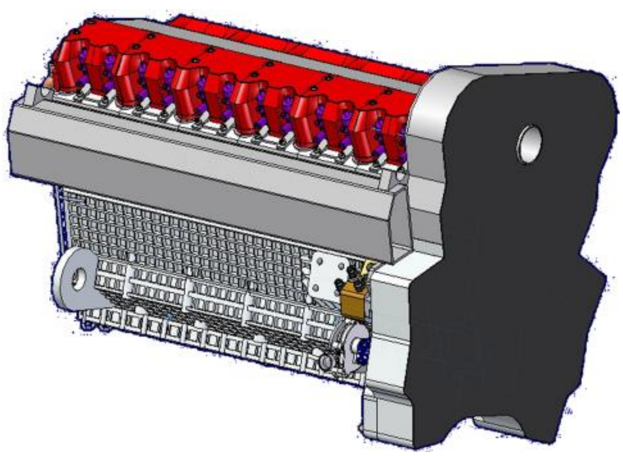

Fig. 2 VD007-II V12, four-stroke engine with a 60 deg bank angle, rated at 2200 HP

2.4 Air Mass Flowrate Estimation.

Accurate estimation of the air mass flowrate is a fundamental aspect of high-power diesel engine design. The airflow directly affects combustion efficiency, turbocharger sizing, intercooling requirements, and FADEC control calibration, especially under transient or high-demand conditions such as takeoff or climb. In the following, a first-order calculation is presented for the VD007 turbocompound engine, illustrating how air mass flow requirements are determined from basic engine parameters and highlighting their relevance for both thermodynamic analysis and practical system integration. The air mass flowrate required by a diesel engine can be estimated based on its mechanical power output, thermal efficiency, air-to-fuel ratio (AFR), and the lower heating value (LHV, also known as PCI) of the fuel. The general expression for the air mass flowrate $\dot{m}_{\text{air}}$, expressed in kilograms per second (kg/s), is given by the following equation:

$$\dot{m}_{\text{air}} = \frac{P}{\eta \cdot \text{PCI}} \cdot \text{AFR} \tag{1}$$

where P is the engine mechanical power output in kilowatts (kW), η is the overall thermal efficiency of the engine (dimensionless), PCI is the lower heating value of the fuel in megajoules per

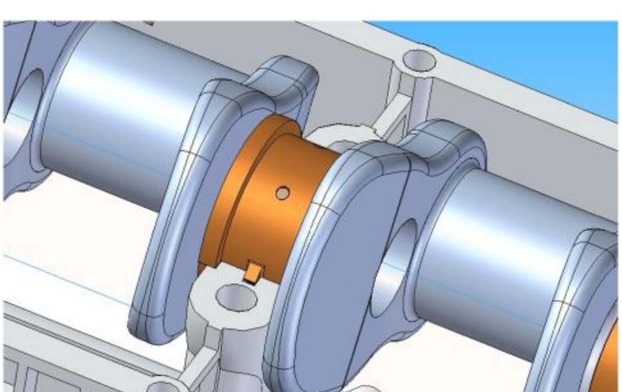

Fig. 3 VD007-II crankshaft detail on the bearing support

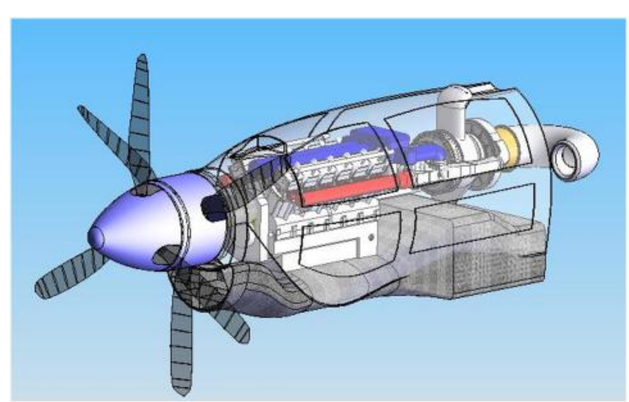

Fig. 4 3930 HP VD007 turbocompound engine coupled with a modified 867 HP Pratt & Whitney Canada PT6 turboshaft installed in the engine nacelle of a Lockheed C-130J

kilogram (MJ/kg), and AFR is the air-to-fuel mass ratio (dimensionless).

We isolate the AFR:

$$\text{AFR} = \dot{m}_{\text{air}} \cdot \frac{\eta \cdot \text{PCI}}{P} \tag{2}$$

Substituting the known values (takeoff turbocompound):

- $\dot{m}_{\text{air}} = 3.6$ kg/s (see Table 5)
- $\eta = 0.30$

$$\text{AFR} = 3.6 \cdot \frac{0.30 \cdot 42 \times 10^6}{1640} \approx 27.65 \tag{3}$$

Thus, for an overall thermal efficiency of 30%, the AFR required to achieve an air mass flowrate of 3.6 kg/s at 2200 HP is approximately 27.65 (VD007 turbocompound – takeoff). It is important to emphasize that the calculated value represents a baseline estimate under takeoff conditions. Variations in engine thermal efficiency, air–fuel ratio, or delivered power will alter the required airflow, demonstrating the sensitivity of the system to operational parameters. Moreover, this estimation serves as a practical reference for the design of auxiliary components and the calibration of the FADEC system, ensuring that the engine maintains optimal combustion, performance, and safety across the full operating envelope. By providing both a numerical example and its practical interpretation, the analysis bridges the gap between theoretical modeling and applied engine design.

3 Results and Discussion

Comparative analyses highlight a persistent efficiency gap between conventional turboshaft engines and modern diesel technologies. While smaller diesel engines have consistently demonstrated superior fuel economy, scaling this advantage to the 1000–5000 shp class remains a major challenge. Automotive-derived conversions and high-performance gasoline-to-diesel adaptations have shown limited applicability due to weight, durability, and power constraints. These limitations provided the rationale for developing a clean-sheet, aviation-grade diesel engine specifically tailored for high-power applications. The VD007 project thus represents an experimental effort to bridge this gap, offering concrete results to evaluate the feasibility of such an approach.

Results confirm that diesel engines, particularly CRDIDs, achieve significantly lower specific fuel consumption and competitive lifecycle costs compared to traditional avgas piston engines. However, despite their efficiency, weight penalties and system complexity limit their suitability as direct replacements for turboshafts. Turboshaft engines retain clear advantages in power-to-weight ratio and reliability, especially under high continuous loads. Nevertheless, benchmarking demonstrates that under partial or off-design conditions, diesel powerplants offer substantial cost savings and extended operational flexibility. Together, these findings frame the evaluation of the VD007 engine, positioning it as a promising yet transitional solution within the broader propulsion landscape.

Paradoxically, the turbocompound system employing a turboshaft as a turbocharger represents the configuration in which the CRDID engine demonstrates its full potential. During takeoff, for a few critical seconds, the propulsion system must deliver maximum power irrespective of fuel efficiency. Under such conditions, it is advantageous to operate the turboshaft, which functions as the compressor for the CRDID, at its maximum rotational speed, achieving a pressure ratio of approximately 6:1. Consequently, the CRDID intake pressure reaches about 6 bar, assuming atmospheric pressure is 1 bar. However, since the maximum allowable pressure in the VD007-II combustion chamber is limited to 300 bar, injection and combustion must be deliberately delayed to preserve peak chamber pressure. This delay significantly reduces the CRDID's thermal efficiency to approximately 30%, resulting in incomplete and soot-rich combustion.

The resulting exhaust gases from the CRDID are then directed into the turboshaft's combustion chamber. This design also allows for a fail-safe mode: in the event of total diesel engine failure, the system can bypass the CRDID and rely on the turboshaft as a backup source of thrust. During takeoff, the CRDID discharges hot, hydrocarbon-laden exhaust gases, which are subsequently postcombusted in the turboshaft burner. This process raises the turbine inlet temperature to its maximum permissible value, effectively recovering energy from unburned fuel and particulates, and enabling the turboshaft to deliver peak power output. The high-temperature, high-mass-flow gases drive the turbine, contributing significantly to total propulsion through the rear-mounted propeller.

Once the takeoff phase concludes, with landing gear and flaps retracted, the system reverts to optimal efficiency conditions, with a boost pressure of approximately 3.4. Under these cruise-oriented operating conditions, the CRDID engine operates closer to its thermodynamically optimal combustion regime. The effective cycle efficiency of the combined turbocharged and turbocompound architecture may then approach values close to 60% under ideal operating conditions.

It should be noted that this value does not correspond to the brake thermal efficiency of the engine alone. For high-performance turbocharged diesel engines, the brake thermal efficiency typically lies in the range of approximately 38–42%, while the indicated efficiency of the combustion process may reach about 48–52% under favorable operating conditions. The higher value approaching 60% refers instead to the theoretical thermodynamic efficiency of the integrated propulsion cycle when accounting for exhaust energy recovery through turbocompounding. In this configuration, a portion of the exhaust energy that would normally be lost is partially converted into additional useful shaft power by the downstream turbine stage, thereby increasing the overall system-level efficiency of the propulsion architecture.

3.1 Finite Element Analysis of VD007 Components.

The dual-injection concept represents a novel approach aimed at improving fuel atomization and combustion efficiency. However, from an industrial perspective, it introduces several notable challenges. These include increased mechanical complexity, higher manufacturing costs, potential durability concerns due to cyclic mechanical loads, and significant heat rejection and thermal stress issues. Understanding these factors is essential for assessing the feasibility and reliability of the design before experimental implementation.

To address these concerns, preliminary finite element method (FEM) analyses were conducted on key engine components to evaluate both mechanical and thermal stresses under peak operating conditions. These analyses provide insights into potential limitations and guide material selection, cooling strategies, and structural optimization.

3.1.1 Piston Finite Element Method Analysis.

The piston of the VD007 engine was analyzed under peak cylinder pressure conditions of 16 MPa, corresponding to the maximum mean effective pressure expected during operation. The base material of the piston is the aluminum alloy GD Al Si 9, which alone cannot withstand the mechanical stresses at the crown and around the combustion chambers. To overcome this limitation, a 3 mm steel coating of 30 WCrV 179 was applied to the piston crown and the surfaces of the dual combustion bowls. This alloy features a tensile strength of 1400 MPa and yield stresses of 1080 MPa at 100 °C and 900 MPa at 300 °C, providing sufficient strength under operational conditions.

Finite element simulations were conducted using a refined tetrahedral mesh in regions surrounding the combustion chambers, where stress concentrations were expected. The results indicate that the reinforced piston crown and bowls are capable of withstanding the applied 16 MPa pressure without failure.

Representative FEM results, including the von Mises stress distribution and the corresponding safety factor, are presented in Figs. 5(*a*) and 5(*b*).

While the crown and combustion bowls exhibited satisfactory mechanical behavior, the analysis revealed a critical region at the piston pin bore, where stress concentrations were significant. Figures 6(*a*) and 6(*b*) show the initial geometry of the pin bore and the corresponding safety factor distribution before any modifications. To mitigate the stress concentration, the geometry of the pin bore and surrounding material was carefully optimized using a fillet and reinforcement profile. The resulting design achieves a more uniform stress distribution and an increased safety factor, as shown in Figs. 7(*a*) and 7(*b*). This comparison clearly demonstrates the effectiveness of the geometric optimization in addressing the critical stress region.

The final piston, including the 3 mm steel coating and optimized pin bore geometry, has an acceptable mass of 2.6 kg, compatible with the reciprocating mass constraints of the engine, while ensuring structural integrity under peak cylinder pressures and providing enhanced safety margins.

3.1.2 Crankshaft Finite Element Method Analysis. Finite element simulations were performed on the VD007 crankshaft to assess its structural integrity under static loading conditions. The maximum equivalent von Mises stress was found to be 1063 MPa, well below the yield strength of 1710 MPa for the 300 M steel, resulting in a static safety factor of 1.6. Considering the effect of load application rate, a factor of 1.25 can be applied, yielding an enhanced safety factor of approximately 2. The maximum deformation was observed in the second crank web, reaching 0.48 mm, primarily due to the bending load applied at this location.

Figure 8 presents the representative FEM results for the crankshaft. Figure 8(*a*) shows the von Mises stress distribution, highlighting critical stress regions, while Fig. 8(*b*) illustrates the maximum deformation under the applied loads. The results indicate that the crankshaft geometry is structurally adequate, and optimization of the web design allows for material and weight savings while maintaining sufficient safety margins.

3.1.3 Finite Element Analysis of the Engine Block. Finite element simulations were conducted on the VD007 engine block to assess its structural integrity under operational loads. The analysis focused on the upper portion of the block, where high stress concentrations were anticipated, such as the cylinder walls, main bearing supports, and crankcase junctions. To reduce

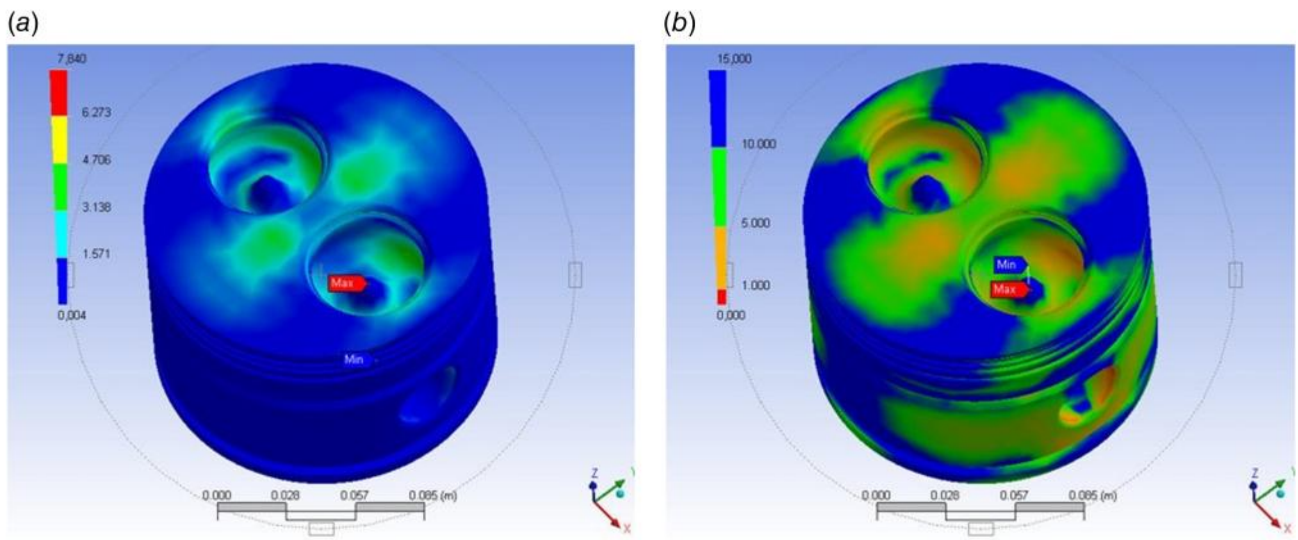

Fig. 5 Initial FEM results for the piston crown and combustion bowls: (*a*)Von Mises stress distribution at 16 MPa and (*b*) safety factor distribution at 16 MPa

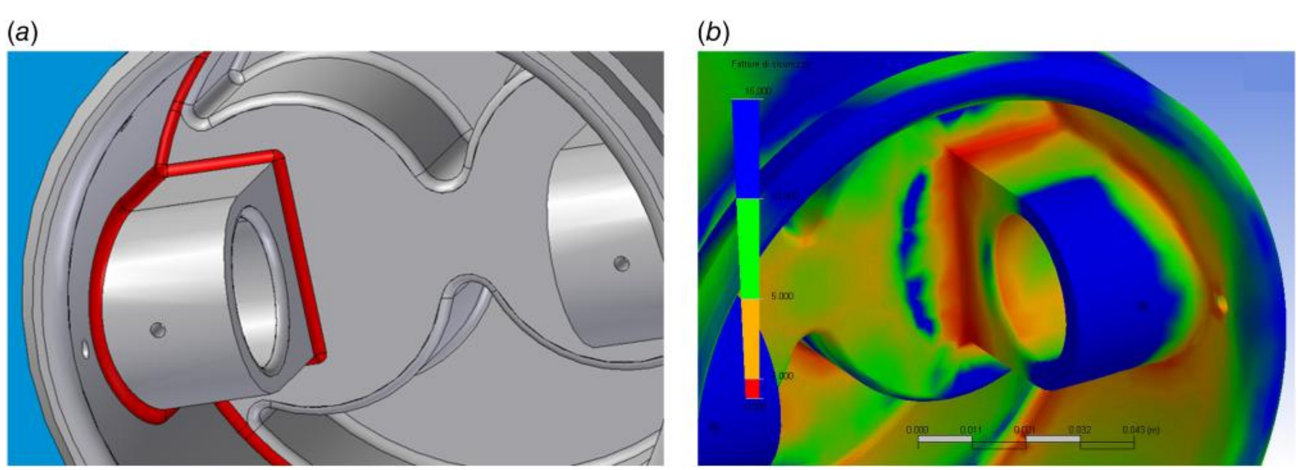

Fig. 6 Piston pin bore region: initial geometry and safety factor distribution highlighting the critical stress area before geometric optimization: (*a*) initial pin bore geometry and (*b*) safety factor before optimization

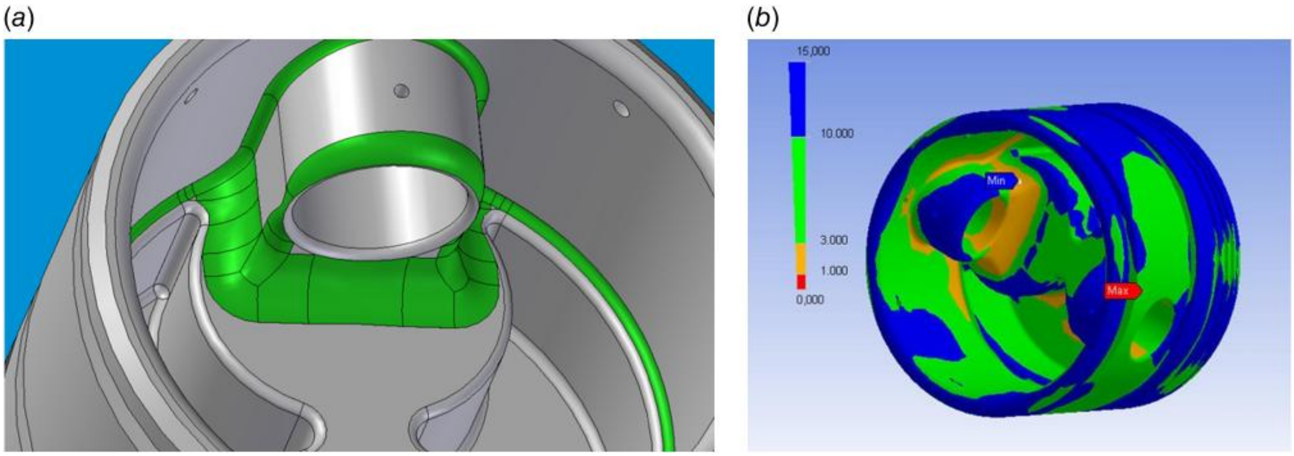

Fig. 7 Piston pin bore region: optimized geometry and resulting safety factor distribution, showing the mitigation of stress concentrations after geometric modification: (*a*) optimized pin bore geometry and (*b*) safety factor after optimization

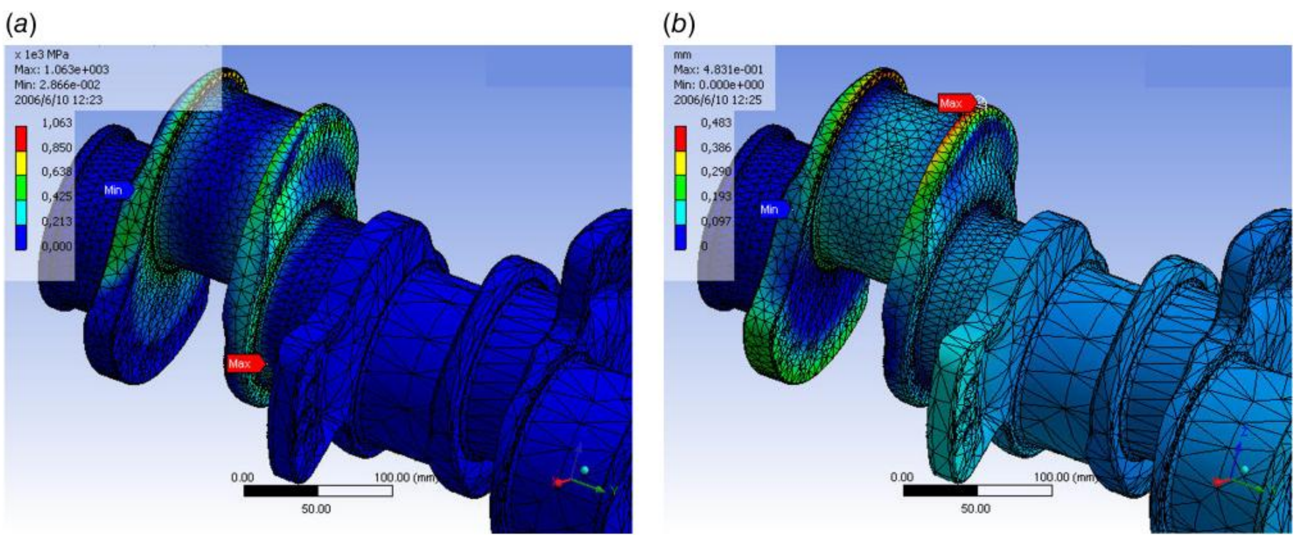

Fig. 8 FEM results of the VD007 crankshaft: (*a*) von Mises stress and (*b*) deformation under static load (mm)

computational complexity, the block was modeled along a longitudinal symmetry plane.

The applied loads included tensile forces from the cylinder head studs, connection bolts of the lower block, and propeller attachment bolts, as well as inertial forces from the crank-piston assembly under 6G acceleration. In addition, the combustion pressure of 190 bar per cylinder was applied.

Initial FEM results indicated that the majority of the block structure met strength requirements. Maximum stresses were observed around the threaded holes for the lower block attachment, which could be mitigated by the use of Helicoil inserts. To further enhance stiffness and improve stress distribution, H-shaped ribs were added along the peripheral walls of the bearing caps. The von Mises stress distribution resulting from the FEM analysis of the engine block is illustrated in Fig. 9.

3.1.4 Summary of Finite Element Method Results. A concise summary of the key numerical results from the FEM analyses is presented here to complement the qualitative stress distributions shown in Figs. 6–9.

For the pistons, the maximum von Mises stress reaches approximately 7.84 MPa. The safety factor before optimization shows values approaching zero in some localized regions, while after structural optimization, the critical zones exhibit a safety factor of about 1, indicating acceptable structural performance under the representative loading conditions adopted in the simulations.

The crankshaft experiences a maximum von Mises stress of approximately 1.063×10^3 MPa, with a maximum deformation of 0.483 mm under the applied loading conditions.

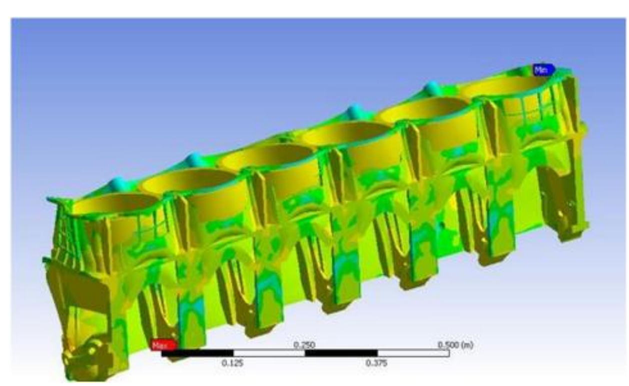

Fig. 9 Von Mises stress distribution of the engine block obtained from FEM analysis

The engine block shows the maximum stress at the threaded region for the lower block fasteners, reaching 3270 MPa. No significant high stress zones are observed elsewhere, indicating the overall structural integrity of the monoblock under the loading scenario considered in the numerical model.

It should be noted that the VD007 combustion chamber is designed to withstand peak cylinder pressures up to approximately 300 bar during extreme operating conditions. However, the finite element analyses presented in this work were conducted using simplified static loading assumptions intended to provide an initial structural feasibility assessment of the main engine components. The adopted boundary conditions therefore represent a conservative but simplified approximation of the complex pressure and load distributions occurring during real combustion events.

In particular, the present analyses do not include thermomechanical coupling effects, transient thermal gradients, or cyclic fatigue loading associated with repeated high-pressure combustion cycles. These phenomena play a critical role in the long-term durability of high-performance compression ignition engines and would require more advanced multiphysics simulations as well as experimental durability validation.

Consequently, the structural results reported here should be interpreted primarily as preliminary engineering evaluations intended to verify the mechanical plausibility of the proposed architecture. A complete structural validation of the VD007 engine would require detailed thermomechanical analyses, fatigue life assessment, and transient loading simulations. Such analyses may lead to more conservative structural dimensions and potentially increased component mass, which would affect the overall power-to-weight ratio of the propulsion system.

Within the scope of the present conceptual study, however, the FEM results provide a useful first-order indication that the main structural components of the VD007 architecture can withstand the representative mechanical loads considered in the simplified model.

3.2 Numerical Engine Simulations. Preliminary thermodynamic simulations of the VD007 V12 engine architecture were conducted using the one-dimensional engine simulation software GT-SUITE. The purpose of these simulations was to evaluate the thermodynamic feasibility of the proposed engine configuration and to obtain an initial estimate of its potential performance under controlled operating conditions.

The numerical model represents a simplified but physically consistent description of the engine system, including the intake and exhaust manifolds, the turbocharging system, the fuel injection process, and the in-cylinder combustion dynamics. Each cylinder was modeled using a single-zone combustion approach, which is commonly adopted in early-stage diesel engine development when the objective is to evaluate overall thermodynamic behavior rather than detailed spatial combustion phenomena.

The principal geometric parameters implemented in the model correspond to the VD007 engine design, including cylinder displacement, compression ratio, valve timing, and fuel injection characteristics. The simulation incorporates the main operational parameters governing diesel engine performance, including the start of injection, injection duration, air–fuel ratio, turbocharger boost pressure, and intake and exhaust valve actuation timing. These parameters were selected to represent nominal full-load operating conditions for a high-performance compression ignition engine.

Boundary conditions were defined assuming standard atmospheric intake conditions, while the turbocharging system was modeled to provide elevated intake manifold pressure consistent with boosted diesel operation. Combustion efficiency and heat release behavior were estimated using standard diesel combustion correlations available within the GT-SUITE modeling environment. Mechanical friction and pumping losses were also considered through empirical correlations typically applied to high-speed compression ignition engines.

To ensure numerical stability and convergence of the solution, each simulation was executed for 300 engine cycles. This duration was selected as a compromise between computational cost and numerical accuracy, allowing the main thermodynamic variables such as cylinder pressure, temperature, and heat release rate to reach periodic steady-state conditions. Once convergence was achieved, the engine performance parameters were extracted from the stabilized solution.

Figure 10 shows the simulated engine power as a function of rotational speed obtained from the numerical model. Under the highly idealized assumptions adopted in the simulation, the numerical scaling of the model yields a theoretical peak power of approximately 36,000 HP at around 5500 rpm. This value does not represent an achievable engine output but rather an artifact of idealized thermodynamic scaling in the absence of realistic mechanical, thermal, turbocharging, and fuel system constraints.

It is important to emphasize that the simulated power levels derive from extrapolating the 4-cylinder terrestrial prototype configuration to a 12-cylinder architecture while neglecting many of the physical limitations that would govern real engine operation. In particular, the simulation assumes ideal combustion efficiency, unrestricted turbocharging capability, and the absence of structural, thermal, and fuel delivery constraints that normally limit achievable engine output.

Experimental testing performed on the four-cylinder VD007 prototype recorded a peak power output of approximately 225–230 HP at 3000 rpm. When extrapolated to a 12-cylinder configuration while accounting for realistic engineering constraints such as mechanical stresses, thermal loading, turbocharger efficiency, and fuel system limitations, the practical design target for the VD007 V12 engine is estimated to be approximately 2200 HP at 3800 rpm.

For this reason, the GT-SUITE simulation results should be interpreted primarily as an exploratory thermodynamic assessment of the engine concept rather than a direct prediction of achievable engine performance. More detailed numerical analyses and additional experimental validation would be required to refine these estimates and to determine the attainable performance limits of the proposed engine architecture.

3.3 Experimental Results and Performance of the VD007 Engine. It should be emphasized that the thermal efficiency values cited herein—potentially approaching 60% under optimized conditions—and the nominal peak output of 2200 HP are derived primarily from preliminary analytical calculations, simulation models, and bench tests conducted on a four-cylinder prototype. These investigations indicate that the engine *could* be optimized for high thermal efficiency, potentially reaching values close to 60% under ideal operating conditions. However, during high-performance regimes, such as maximum power output during takeoff, thermal efficiency is expected to be lower, in the range of 45–50%, according to theoretical considerations. In practice, actual operational efficiency is likely to remain below these theoretical estimates.

The experimental bench tests were carried out on a four-cylinder prototype derived from the VD007 double-injection diesel concept, fabricated and tested at Oral Engineering S.R.L., Baggiovara (MO), Italy. This prototype preserves the essential features of the double-injection diesel architecture, including dual injectors per cylinder, while allowing comprehensive preliminary validation on a smaller, more manageable scale.

The main structural parameters of the four-cylinder test engine are as follows:

- Number of cylinders: 4
- Bore: 110 mm
- Stroke: 118.5 mm
- Connecting rod length: 212.8 mm

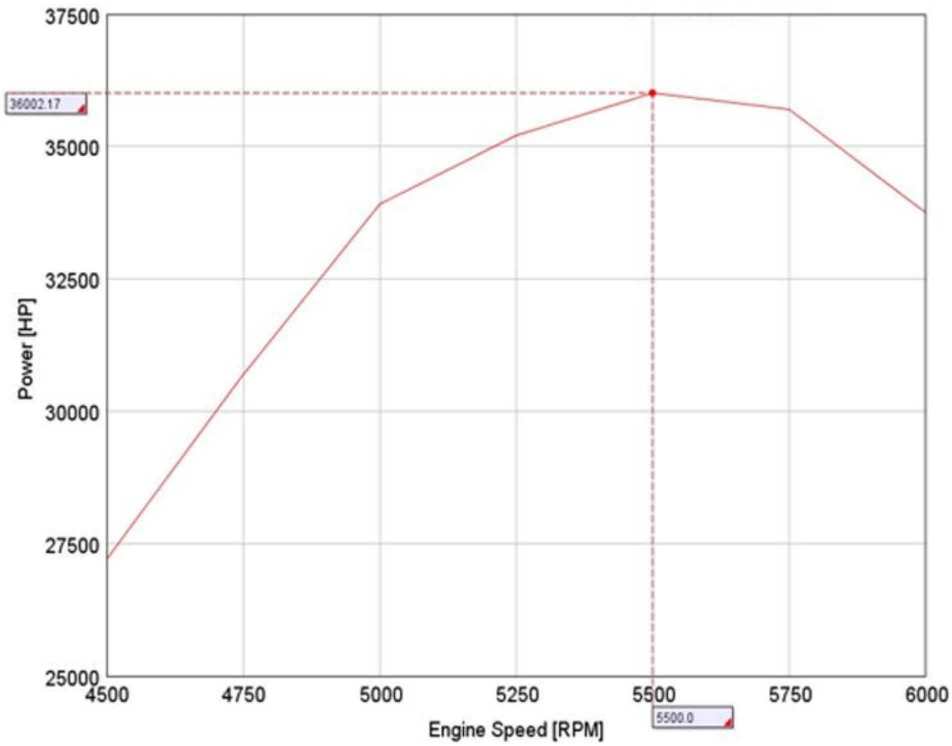

Fig. 10 Idealized GT-SUITE simulation of engine power as a function of rotational speed for the VD007 V12 architecture. The extremely high-power values result from thermodynamic scaling under ideal assumptions and do not represent achievable engine performance.

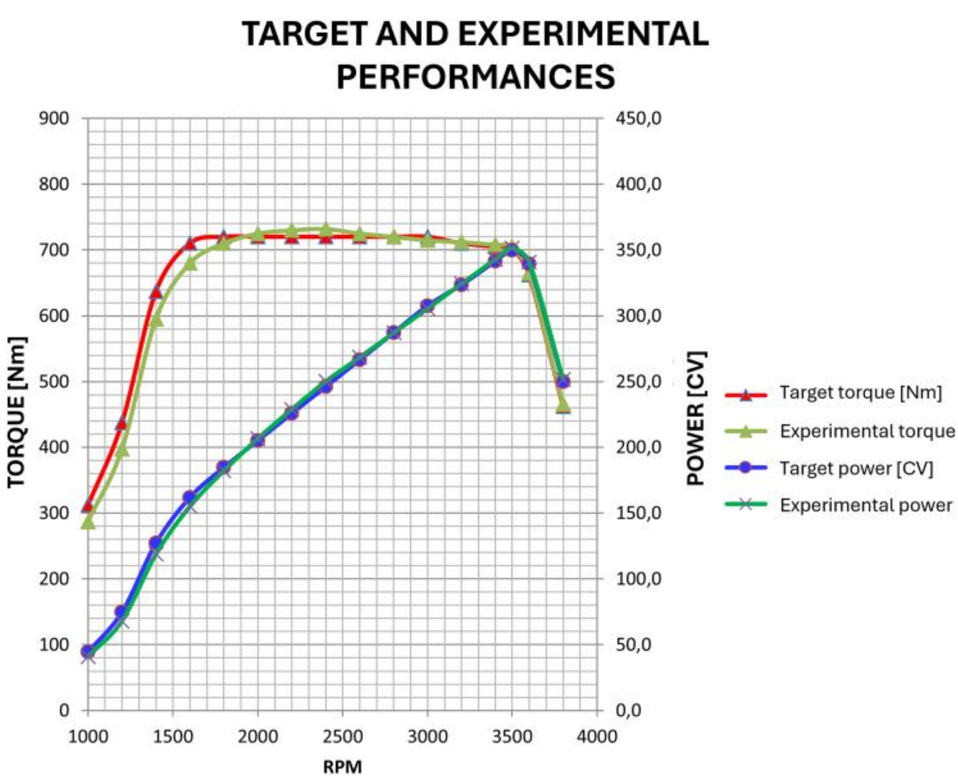

Fig. 11 Torque and power curves of the four-cylinder VD007 test engine, measured at medium-to-high loads

- Maximum engine speed: 3800 rpm

Torque and power curves were recorded during test bench operations, as illustrated in Fig. 11. All tests were carried out in accordance with ISO 1585:2020, which defines procedures for measuring net engine power under controlled laboratory conditions.

The four-cylinder prototype demonstrated a torque plateau ranging approximately from 1500 to 3500 rpm, with a peak

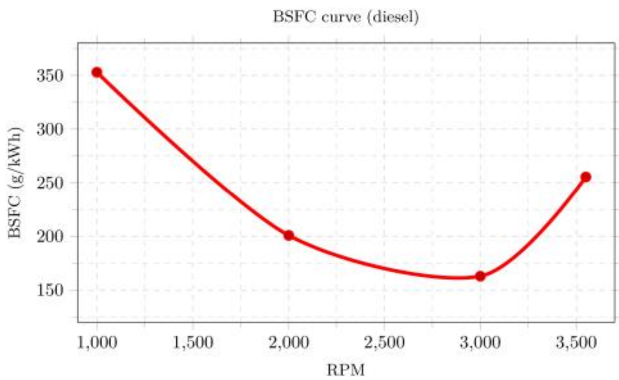

Fig. 12 BSFC curve for diesel (LHV = 42.5 MJ/kg)

torque of about 700 Nm. Power output increased from 50 HP at 1000 rpm to roughly 200 HP at 2000 rpm, reaching a maximum of 350 HP near 3500 rpm. The corresponding BSFC was measured using an AVL Plutron flowmeter along the low-pressure fuel line, with recirculation of fuel returning from the injectors to ensure only the diesel effectively drawn from the tank was accounted for.

Figure 12 shows the BSFC curve across the tested RPM range, varying from approximately 353 g/kWh at 1000 rpm down to a minimum of 163 g/kWh around 3000 rpm, rising again to 255 g/kWh near 3550 rpm at higher loads. At its best measured point (3000 rpm, 163 g/kWh), the prototype demonstrates efficiency comparable to state-of-the-art heavy-duty automotive diesels (∼185–195 g/kWh).

It is emphasized that the 4-cylinder prototype validates only specific aspects of the VD007 V12 design, including achievable BSFC, combustion concept, and dual-injector operation. Full-scale V12 validation, including long-term durability, high-altitude operation, and turbocompound integration, remains untested; results for the V12 are therefore projected based on simulation and analytical models.

The VD007-III features a further reduced stroke to achieve a maximum engine speed of 7000 rpm, enabled by the use of more advanced and higher performance common rail injectors. The V12 engine will not be fully developed beyond the preliminary design phase, as it has been superseded by two-stroke diesel engines, for which an introductory article is currently in preparation. In its maximum configuration, the VD007-II arranged in an H24 layout would develop approximately 4000 HP, representing the design limit of the project. The H24 configuration has never been studied.

The four-stroke VD007 CRDID, even in its most advanced configuration, has proven unable to validly replace gas turbines. Despite its high thermal efficiency and the logistical advantages associated with the use of diesel or Jet-A fuel, the engine suffers from excessive bulk and an unfavorable power-to-weight ratio. Notably, when compared to representative high-power turboshaft engines such as the Pratt & Whitney PT6A-67D (1200 shp, 200 kg dry weight) or the T700/GE CT7-2E1 (2000 shp, 350 kg dry weight), the VD007 exhibits a substantially higher mass per unit of power, reflecting inherent limitations in scaling four-stroke diesel technology to turboshaft-class outputs. Even the turbocompound variant, designed to recover additional shaft power from exhaust energy and enhance operational flexibility, cannot fully offset this disadvantage in power-to-weight ratio.

Across engine classes, piston-based diesels like the VD007 offer clear advantages in fuel efficiency, lifecycle costs, and compatibility with globally available fuels, particularly at low- to mid-power ranges. High-power turboshafts, in contrast, provide superior continuous power output, higher specific power, and optimized performance under sustained high-load operation, albeit at significantly higher acquisition and operating costs. *Cost per horsepower-hour* metrics further emphasize this trade-off: while the VD007 can achieve competitive operating efficiency, turboshafts remain unmatched in power density, which is critical for rotorcraft and turboprop applications.

As a result, the VD007 program was redirected to Oral Engineering for adaptation as a propulsion unit for ground-based military vehicles. In this application, the stroke has been slightly increased and the bore slightly reduced to improve low-rpm torque. The TBO for this conventional engine, constructed in grey cast iron, exceeds 10,000 h. The aircraft CRDID development program continues, now focusing on a two-stroke diesel concept, which appears to offer greater promise for future high-power aviation applications, potentially bridging the gap between piston diesel efficiency and turboshaft-level power density.

It is important to note that the experimental four-cylinder VD007 prototype was built in an inline configuration, effectively representing a single bank of the V12 architecture. The measured torque and power curves validate the dual-injection strategy, demonstrating stable combustion and efficient energy release under real operating conditions. These results provide a sound basis for scaling to the 12-cylinder configuration: the experimental inline prototype not only validates the dual-injection system but also serves as a reference for expected performance of the full V12 engine. While the four-cylinder prototype achieved a peak output of 225–230 HP at 3000 rpm, the V12 layout, accounting for practical limits on structural strength, thermal management, and fuel delivery, yields a realistic design target of approximately 2200 HP at 3800 rpm. Therefore, the inline four-cylinder prototype effectively bridges experimental data and simulation predictions for the V12 engine, addressing both the combustion concept and the achievable performance.

3.3.1 Certification Considerations for Aviation Diesel Engines. The transition of the VD007 engine from experimental prototype to certified aviation powerplant requires compliance with stringent regulatory frameworks, including the European Union Aviation Safety Agency (EASA) and the Federal Aviation Administration (FAA) standards. Key certification challenges for high-power diesel engines include: verification of combustion stability and emissions across the full flight envelope, structural and fatigue assessment of the reinforced engine block and turbocharging systems under continuous high-load operation, thermal management validation under extreme ambient conditions, and full FADEC reliability and redundancy testing. Additionally, compliance with fuel system safety standards, vibration and torsional oscillation limits, and acoustic noise regulations must be demonstrated. Certification testing mandates a structured program comprising component-level tests, full-engine bench runs, and flight trials to substantiate endurance, reliability, and performance margins. The unique characteristics of turbocharged and turbocompounded diesel architectures necessitate detailed documentation and justification for all deviations from established turbine and spark-ignition engine certification precedents, potentially extending the certification timeline and development cost.

4 Conclusions

This study investigated the feasibility and performance potential of high-power diesel engines for aviation through a combination of benchmarking, analytical modeling, numerical simulations, and experimental evaluation on a prototype engine. Comparative analysis with conventional piston engines (e.g., Continental CD-170, Lycoming O-360) and low- to high-power turboshafts (e.g., Pratt & Whitney PT6A, Rolls-Royce AE 2100) allowed a quantitative assessment of the potential advantages and limitations of the proposed VD007 architecture.

The VD007 represents a technically innovative clean-sheet V12 Common Rail Diesel Injection Engine (CRDID) designed for the 1000–4000 shp class. Key architectural features include a short-stroke configuration, dual injectors per cylinder, FADEC-controlled turbocharging, and a turbocompound layout enabling partial exhaust energy recovery. The modular design also allows adaptation to different applications, including terrestrial and high-torque low-RPM variants.

Performance estimates for the V12 configuration were obtained through analytical modeling and numerical simulations of the complete architecture. These analyses suggest that a practical peak output on the order of 2200 HP may be achievable for the proposed V12 configuration when realistic mechanical, thermal, and turbocharging constraints are considered. The simulations also indicate high potential thermal efficiency and an estimated air mass flowrate of approximately 3.6 kg/s under takeoff operating conditions.

The numerical thermodynamic simulations conducted with the GT-SUITE model also provide useful insight into the scaling behavior of the proposed architecture. While idealized simulations suggest that very high theoretical power levels may be obtained when extrapolating the prototype configuration, the introduction of realistic structural, thermal, and turbocharging constraints significantly reduces the achievable performance. This behavior highlights the practical engineering limits encountered when scaling high-speed diesel architectures to very high power levels for aviation propulsion.

Experimental validation was performed on a terrestrial inline four-cylinder prototype derived from the VD007 architecture, manufactured at Oral Engineering S.p.A. in Baggiovara (MO), Italy. Tests were conducted according to ISO 1585:2020 procedures. The experimental campaign recorded a minimum brake-specific fuel consumption of 225 g/kWh at medium-to-high loads. Torque and power curves obtained during these tests provide empirical support for the dual-injection combustion concept and the general operating behavior of the architecture. Fuel flow was measured using an AVL Plutron system to ensure accurate determination of injected fuel quantities.

In comparison, conventional piston engines typically deliver 150–300 HP with specific operating costs of 0.32–0.51 USD/(hp·h), while low- and high-power turboshafts achieve 750–4800 shp with Cost/(hp·h) in the range 0.31–0.67 USD/(hp·h). These figures highlight the potential efficiency advantages of diesel architectures relative to traditional piston engines, while also emphasizing the remaining challenges in terms of power-to-weight ratio and system integration when compared with modern turboshaft engines.

Despite these challenges, the VD007 program provides valuable insights into high-power aviation diesel architectures. The results demonstrate the feasibility of dual-injector combustion strategies, FADEC-controlled turbocharging, and turbocompound energy recovery, while offering a reference framework for modular and scalable engine layouts. For terrestrial applications, the architecture has already been implemented in inline four-cylinder and two-cylinder hybrid configurations optimized for low-RPM torque.

Future research aimed at aviation applications will focus on combustion optimization, emissions characterization, structural reliability, and further development of lightweight architectures, including potential two-stroke diesel concepts to improve power-to-weight ratios. Additional work will also be required to assess compliance with EASA and FAA certification requirements.

Taken together, these results define the main scientific contributions of the present study: a quantitative benchmarking across different aircraft propulsion architectures, experimental demonstration and partial validation of the dual-injection diesel concept, and a realistic assessment of the limitations encountered when scaling four-stroke diesel engines to high-power aviation applications. The study therefore highlights both the potential and the current limitations of compression ignition propulsion systems in future aviation powerplant development.

Conflict of Interest

There are no conflicts of interest. This article does not include research in which human participants were involved. Informed consent not applicable. This article does not include any research in which animal participants were involved.

Data Availability Statement

No data, models, or code were generated or used for this paper.

Appendix: Detailed Benchmarking and Cost Analysis of Aircraft Propulsion Systems

This section introduces the approach for systematically comparing different aircraft propulsion systems, ranging from traditional gasoline piston engines to modern diesel and turboshaft alternatives. Key performance metrics, operating costs, and maintenance philosophies are examined to provide a comprehensive baseline. The subsequent sections detail technical specifications, cost evaluations, and maintenance considerations, highlighting trade-offs between efficiency, reliability, and lifecycle economics across power classes and engine types.

Comparison of Common Piston Aircraft Engines. Tables 6 and 7 summarize the technical and economic characteristics of conventional gasoline engines (Lycoming, Continental), modern diesel powerplants (Austro AE300, Continental CD series), and lightweight Rotax models. Table 6 reports fuel type, TBO/TBR, rated power, and dry weight, while Table 7 provides purchase price, estimated operating cost per flight hour, and normalized cost per horsepower-hour.

The data reveal key trends in the current piston engine market. Traditional avgas engines, such as the Lycoming O-360 and Continental IO-550, offer established reliability and relatively high power, but incur higher fuel consumption and operating costs per unit of power. Lightweight engines like the Rotax 912 ULS provide low weight and cost, suitable for light sport and ultralight aircraft, at the expense of absolute power. Diesel engines, including the Continental CD and Austro AE300 series, achieve superior fuel efficiency and competitive lifecycle costs, thanks to higher thermal efficiency and Jet-A fuel use, though they generally have greater dry weight and initial cost.

Combining technical and economic metrics enables comparison across power classes and engine types. Smaller diesel engines deliver significant savings per horsepower, but scaling to higher power levels introduces challenges in weight, durability, and integration. These observations provide context for evaluating the

Table 6 Technical specifications of selected piston aircraft engines used as reference cases in this study

Engine model	Fuel type	TBO/TBR (h)	Power (hp)	Dry weight (kg)
Lycoming O-360	AvGas (100LL)	2000	180	115
Continental IO-550	AvGas (100LL)	2000+	310	190
Rotax 912 ULS	MoGas/AvGas	1200–1500	80–100	63
Continental CD-170	Jet-A/diesel	1200–1800[a]	170	156
Austro AE300/ CD-155	Jet-A (diesel)	2000–2400	155	185
Continental CD-300	Jet-A (diesel)	3000	300	255
VD007 (V12)	Jet-A/diesel	3000–3500	2143	287

Note: Performance parameters and technical data are derived from manufacturer specifications and publicly available technical documentation. The values reported for the VD007 engine correspond to design estimates and analytical projections presented in this work. Values are approximate and may vary by configuration.
[a]Initial TBR of 1200 h, increased to 1800 h for the CD-170.

Table 7 Updated cost estimates for selected piston aircraft engines

Engine Model	Price (USD)	Operating Cost/ hr (USD)	Cost/(hr·hp) (USD)
Lycoming O-360	\$28,000–32,000	\$92.25	\$0.51
Continental IO-550	\$60,000–70,000	\$147.75	\$0.48
Rotax 912 ULS	\$23,000–25,000	\$43.00	\$0.43
Continental CD-170	\$80,000–100,000[a]	\$60.44	\$0.36
Austro AE300 / CD-155	\$65,000–70,000	\$61.20	\$0.40
Continental CD-300	\$90,000–100,000	\$94.67	\$0.32
VD007 V12	\$400,000–450,000	\$425	\$0.198

Note: Engine prices are based on publicly available market data and typical vendor quotations, while operating cost and cost/(h·hp) values are estimated using the methodology described in Section "Calculation of Specific Operating Cost per Horsepower-Hour," including fuel consumption, overhaul reserve, scheduled maintenance, and miscellaneous operating costs. The values reported for the VD007 engine correspond to design-based estimates developed in this study.

[a]Initial TBR of 1200 h, increased to 1800 h for the CD–170. Values are estimated based on cruise fuel flow, average fuel price (2025), and maintenance reserves.

feasibility and advantages of high-power aviation diesel engines, forming a basis for discussion of the CRDID and VD007 projects.

The relatively low estimated dry weight of the VD007 V12 engine (approximately 287 kg for a 20 L displacement) results from a combination of design and material choices aimed at achieving high power density. The engine block and cylinder heads are constructed from high-strength aluminum alloys with selective steel reinforcement in critical areas, while connecting rods and pistons utilize forged aluminum and titanium alloys, respectively. Component geometry has been optimized using finite element–informed topology techniques, allowing material reduction in low-stress regions without compromising structural integrity. A short-stroke configuration and compact packaging reduce overall block volume, and integrated passages for oil and coolant further decrease mass. Certain peripheral systems, such as accessory drives and cooling jackets, are represented in the preliminary design by simplified mass equivalents rather than full assemblies, consistent with typical design-phase weight estimation practices. Component-level weight estimates are approximately: engine block 120 kg, cylinder heads 40 kg, crankshaft 35 kg, turbocharging and intake/exhaust systems 25 kg, and remaining auxiliaries and housings 67 kg, summing to the total dry weight. Collectively, these strategies produce a design mass lower than conventional diesel engines of similar displacement, while maintaining the high power-to-weight ratio required for aviation applications.

Calculation of Specific Operating Cost per Horsepower-Hour. The specific operating cost per horsepower-hour, denoted as Cost/(h · hp), represents the marginal cost to operate the engine per unit of power output over time. This metric is fundamental for performance and cost-efficiency evaluations across different engine types.

The specific cost is calculated by dividing the total hourly operating cost by the rated engine power:

$$\text{Cost}/(\text{h}\cdot\text{hp}) = \frac{C_{\text{total}}}{P} \tag{A1}$$

where C_{total} is the total hourly operating cost (in USD/h), comprising several components:

$$C_{\text{total}} = C_{\text{fuel}} + C_{\text{overhaul}} + C_{\text{maintenance}} + C_{\text{misc}} \tag{A2}$$

with

- C_{fuel}: Hourly fuel cost (USD/h), calculated as the product of fuel consumption rate and fuel price.
- C_{overhaul}: Overhaul reserve cost per hour (USD/h), obtained by dividing the total overhaul cost by the engine's TBO or TBR. Example values from the three engines considered are as follows:

$$\begin{cases} 300\,\text{USD/h} & \text{Rolls-Royce AE2100(TBO} = 5000\,\text{h, overhaul cost} = 1,500,000\,\text{USD)} \\ 19.44\,\text{USD/h} & \text{Continental CD} - 170\text{(TBR} = 1800\,\text{h, overhaul cost} = 35,000\,\text{USD)} \\ 10.00\,\text{USD/h} & \text{Lycoming O} - 360\text{(TBO} = 2000\,\text{h, overhaul cost} = 20,000\,\text{USD)} \end{cases}$$

- $C_{\text{maintenance}}$: Scheduled maintenance cost per hour (USD/h). Example values are as follows:

$$\begin{cases} 150\,\text{USD/h} & \text{Rolls-Royce AE2100} \\ 6.00\,\text{USD/h} & \text{Continental CD-170} \\ 8.00\,\text{USD/h} & \text{Lycoming O-360} \end{cases}$$

- C_{misc}: Consumables and miscellaneous operating costs per hour (USD/h). Example values are as follows:

$$\begin{cases} 50\,\text{USD/h} & \text{Rolls-Royce AE 2100} \\ 2.00\,\text{USD/h} & \text{Continental CD-170} \\ 3.00\,\text{USD/h} & \text{Lycoming O-360} \end{cases}$$

- P is the rated power output of the engine in horsepower (hp).

Fuel prices are commonly expressed in USD per gallon but can be converted to USD per kilogram using the following relation:

$$C_{\text{fuel,kg}} = \frac{C_{\text{fuel,gal}}}{\rho} \tag{A3}$$

where $C_{\text{fuel,kg}}$ is the fuel cost per kilogram (USD/kg), $C_{\text{fuel,gal}}$ is the fuel cost per gallon (USD/gal), and ρ is the fuel density in kilograms per gallon (kg/gal).

Typical fuel densities used for the conversion are as follows:

- Avgas (100LL): $\rho = 6.01$ lb/gal = 2.73 kg/gal
- Gasoline (automotive): $\rho = 6.3$ lb/gal = 2.86 kg/gal
- Diesel (ULSD): $\rho = 7.1$ lb/gal = 3.22 kg/gal
- Jet-A fuel: $\rho = 6.8$ lb/gal = 3.09 kg/gal

Note that 1 lb = 0.4536 kg has been used for conversion.

For example, for Jet-A fuel priced at 6.00 USD/gal, the cost per kilogram is given as follows:

$$C_{\text{fuel,kg}} = \frac{6.00\,\text{USD/gal}}{3.09\,\text{kg/gal}} \approx 1.94\,\text{USD/kg} \tag{A4}$$

This conversion enables direct comparison when fuel consumption is reported by mass rather than volume. The calculations assume continuous operation at full rated power, which simplifies standardization but does not capture partial-load operation typical in real conditions. Off-design operation can cause nonlinear variations in fuel use, thermal efficiency, and maintenance needs, affecting the calculated specific operating cost.

Fuel price fluctuations also impact the hourly cost, and sensitivity analyses are recommended to evaluate different market scenarios. The cost parameters are based on manufacturer data, empirical observations, and industry averages [17]. Breaking down costs into fuel, overhaul, scheduled maintenance, and miscellaneous components enhances transparency and supports benchmarking across engine types, providing a solid basis for evaluating efficiency, operational economics, and performance.

Sensitivity of Cost Metrics to Fuel Price and Specific Fuel Consumption: Because fuel cost represents a significant portion of the total operating cost, variations in fuel price and SFC can influence the calculated cost metrics. A qualitative sensitivity analysis was therefore performed to assess how moderate variations in these parameters affect the resulting cost-per-hour and cost/(hp·h) values.

If fuel price varies by approximately ±20%, the fuel cost component C_{fuel} changes proportionally, producing a corresponding shift in the total hourly operating cost C_{total}. Since turbine engines typically exhibit higher SFC values than compression-ignition engines, increases in fuel price tend to amplify the relative operating cost advantage of diesel architectures.

Similarly, a ±20% variation in SFC directly modifies the fuel flowrate and therefore the hourly fuel cost. While this variation affects all engine types, engines with lower baseline SFC remain comparatively less sensitive to fuel price fluctuations in terms of cost per horsepower-hour.

Although the numerical values presented in this work are based on nominal parameters representative of current market conditions, these sensitivity considerations indicate that the relative economic comparison between diesel piston engines and turboprop/turboshaft engines remains broadly consistent across realistic variations in fuel price and fuel consumption.

Table 8 Technical specifications of "low-power" turboshaft aircraft engines

Engine model	Fuel type	TBO (h)	Power (shp)	Dry weight (kg)
Rolls-Royce M250-C20B	Jet-A	3,500	~420	~62
Pratt & Whitney PT6A-34	Jet-A	3,600–4,000	~750	~180
Safran Arriel 2D	Jet-A	4,000	~950	~210
GE CT7-8A	Jet-A	4,000–5,000	~2000	~380
Allison 250-C30	Jet-A	3,500	~650	~90

Table 9 Cost-related data of "low-power" turboshaft aircraft engines, including estimated cost per hour per horsepower

Engine model	Price (USD)	Operating cost/h (USD)	Cost/(h·shp)
Rolls-Royce M250-C20B	$300,000–400,000	$250–300	$0.60–0.71
Pratt & Whitney PT6A-34	$500,000–650,000	$400–500	$0.53–0.67
Safran Arriel 2D	$600,000+	$500–600	$0.53–0.63
GE CT7-8A	$1.5M+	$900–1100	$0.45–0.55
Allison 250-C30	$350,000–450,000	$300–350	$0.46–0.54

Note: Cost/(h·shp) calculated using estimated average power output. Costs include fuel and maintenance.

Comparison of Common "Low-Power" Turboshaft Aircraft Engines. Tables 8 and 9 provide a comparative summary of selected turboshaft aircraft engines, focusing on their technical and economic characteristics. The "Operating Cost per Hour" includes estimated fuel burn and engine reserve costs, derived from published data and manufacturer sources. Turboshaft engines are primarily used in rotary-wing aircraft and high-performance light aircraft, offering high power-to-weight ratios but at significantly higher acquisition and operating costs compared to piston engines.

Instead, the comparison in Tables 6 and 7 illustrates trade-offs among traditional avgas engines, modern diesels, and lightweight Rotax models. Lycoming and Continental engines offer proven reliability and service support but incur higher operating costs due to fuel consumption and avgas pricing. Diesel engines, including the Continental CD and Austro AE300 series, achieve lower fuel costs and longer TBR intervals, offsetting higher purchase prices and complexity. Rotax engines provide low operating cost and weight for light sport aircraft but deliver limited power and shorter TBO. Engine choice depends on operational profile, regulatory constraints, and fuel availability, with diesels increasingly attractive for efficiency and global fuel access, while avgas engines remain dominant in certified general aviation.

Cost Comparison Between "Low-Power" Turboshaft and Piston Engines. Turboshaft and piston engines offer distinct trade-offs in aircraft propulsion. Piston engines, such as the Continental CD-170 or Rotax 912 ULS, achieve low hourly operating costs ($40–$100/h) and are suited for low-speed, low-altitude applications in general aviation and light aircraft. Turboshafts, like the Rolls-Royce M250 or Pratt & Whitney PT6A, provide higher power-to-weight ratios and thermal efficiency under continuous high-load operation, but incur much higher operating costs ($300–$1,000/h) due to fuel, complexity, and expensive maintenance. Cost per horsepower-hour further highlights piston engines' efficiency at lower outputs ($0.32–$0.51/hp·h) versus turboshafts ($0.45–$0.70/hp·h). Engine selection thus depends on balancing performance needs with long-term operational economy, with pistons favored for cost-sensitive, light-aircraft roles, and turboshafts for high-performance or rotorcraft applications.

Comparison of High-Power Turboshaft Aircraft Engines. Tables 10 and 11 provide a comparative overview of selected high-power turboshaft engines used in rotorcraft and turboprop applications. These engines, typically ranging from 800 to 5000 shaft horsepower (shp), are designed for demanding military, commercial, and utility operations. The "Operating Cost per Hour"

Table 10 Technical specifications of representative high-power turboshaft aircraft engines (approx. 800–5000 shp) used as reference cases in this study. Performance parameters and technical data are derived from manufacturer specifications and publicly available technical documentation. Values are approximate and may vary depending on configuration and application

Engine Model	Fuel Type	TBO (h)	Power (shp)	Dry Weight (kg)
Pratt & Whitney PT6A-67D	Jet-A	3,600–4,000	1,200	200
General Electric CT7-2E1	Jet-A	4,000	2,000	350
Rolls-Royce AE 2100	Jet-A	5,000	4,600	585
Klimov TV3-117VM	Jet-A	2,000–3,000	2,200	330
Honeywell T55-GA-714A	Jet-A	3,000–4,000	4,800	650
Safran Makila 2A1	Jet-A	4,000	1,800	215

Table 11 Comparison of representative high-power turboshaft aircraft engines (approximately 800–5000 shp) Note: Technical specifications are derived from manufacturer documentation and publicly available technical sources. The cost/(h·hp) values are estimated using the operating cost methodology described in the Materials and Methods section, assuming a representative specific fuel consumption of 0.45 lb/(hp·h). Values are intended for comparative benchmarking and may vary depending on configuration and operating conditions

Engine model	TBO (h)	Power (shp)	Dry weight (kg)	Cost/(h·hp) (USD)
Pratt & Whitney PT6A-67D	3800	1200	200	0.550
General Electric CT7-2E1	4000	2000	350	0.474
Rolls-Royce AE 2100	5000	4600	585	0.457
Klimov TV3-117VM	2500	2,200	330	0.533
Honeywell T55-GA-714A	3500	4800	650	0.490
Safran Makila 2A1	4000	1800	215	0.482

includes estimated fuel consumption and engine reserve based on published technical and operator data.

Assumptions for Cost per Hour Calculation (High-Power Turboshafts). The following assumptions were made in calculating the operating cost per horsepower for the turboprop and turboshaft engines listed in Table 10. These assumptions, consistent with typical values for high-power turboshaft engines, were derived from published data and representative operational parameters reported in the literature and industry sources to ensure transparency and consistency in the analysis:

- *Fuel Burn Rate*: A typical fuel burn rate of 0.45 lb/h per horsepower was assumed for each engine, which is a representative value for high-power turboprop and turboshaft engines. According to Johnson [18], typical SFC values for medium- to high-power turboshaft engines range between 0.35 and 0.50 lb/(hp·h), depending on engine configuration and operating conditions. More recent analyses, such as Yüksel et al. [19], report comparable results for regional turboprop engines, with cruise SFC values in the 0.40–0.47 lb/(hp·h) range. Boito and Benini also confirm similar performance levels in next-generation hybrid-electric propulsion studies. Based on the overall agreement among these independent sources, an average value of 0.45 lb/(hp·h) was selected as a representative assumption for cost estimation.
- *Fuel Cost*: The cost of Jet-A fuel was assumed to be 0.90 USD/lb, consistent with current industry pricing. This value corresponds approximately to 2.00–2.10 USD/kg or 6.00 USD/gal, in line with current global averages reported by AirNav [20], IATA [21], and the U.S. Energy Information Administration (EIA) [22]. Short-term market variations exist, but this figure reflects the stable 2024–2025 price range observed across North America and Europe.
- *Overhaul Cost*: The overhaul cost for each engine was estimated based on a proportional relationship to the engine's power rating. The Pratt & Whitney PT6A-67D, with a base overhaul cost of 485,000 USD for 1200 shp, was used as a reference.
- *Time Between Overhaul*: For high-power turboshaft engines, a TBO interval of 2000–5000 h was assumed. This range is consistent with manufacturer data for comparable turboprop and turboshaft engines, such as the Pratt & Whitney PT6A-114, which reports a basic industry TBO of approximately 3600 h [23].
- *Scheduled Maintenance*: An average scheduled maintenance cost of 100 USD per operating hour was assumed for all engines. This value represents a cautious estimate, accounting for regular inspections, routine parts replacement, and standard maintenance tasks typically performed between major overhauls.
- *Consumables and Miscellaneous*: A cost of 30 USD per operating hour for consumables (e.g., lubricants, filters) and miscellaneous expenses was included. This assumption is consistent with historical cost breakdowns for medium-class helicopters, where lubricants typically represent about 3% of fuel costs and other small supplies and in-flight expenses contribute a similar amount [24].
- *Cost per Hour per Horsepower*: The final cost per hour per horsepower (USD/(hour·hp)) was calculated by dividing the total operating cost (including fuel, overhaul, maintenance, and consumables) by the engine's power rating (in shp).

These assumptions are based on typical operational conditions for commercial and military turboshaft engines, and provide an estimate for the marginal operating cost of delivering power over time.

The data presented in Table 11 highlight key technical and economic characteristics of high-power turboshaft engines used in both rotary- and fixed-wing applications. These engines range from approximately 1200 to 4800 shaft horsepower, power medium to heavy-lift helicopters (e.g., CH-47 Chinook, NH90, Mi-17) as well as regional turboprop aircraft (e.g., C-130J, C295). Despite their significant performance capabilities, the operating costs of these engines remain high, typically between $450 and $1,600 per flight hour. This reflects both their elevated fuel consumption and high engine reserve costs associated with complex components and demanding maintenance standards. For instance, the Rolls-Royce AE 2100 and Honeywell T55 series offer high power outputs exceeding 4000 shp, but at the cost of both increased dry weight and hourly expenditure. Turboshaft engines with moderate output, such as the PT6A-67D and Makila 2A1, offer a compromise between efficiency and capability, making them attractive for light-to-medium utility platforms. Notably, the TBO values range from 2000 to 5000 h, indicating substantial variation in lifecycle planning and overhaul economics among manufacturers and engine families. Overall, the selection of a turboshaft engine in this power class is highly dependent on mission requirements, including payload, altitude, and endurance, and must balance acquisition cost, fuel logistics, and long-term supportability. The operating environment and mission time—particularly in military or offshore applications—often justify the high operational costs through performance and reliability gains.

Maintenance Philosophy: Automotive Diesel Versus Turboshaft Engines. In modern automotive diesel engines, the typical TBR is approximately 4500 h, corresponding to about 250,000 km of on-road operation. Particularly for pre-Euro 5 engines (e.g., Euro 3–4), scheduled maintenance is relatively limited and generally includes periodic oil and filter changes, external component replacement, and electronic fault monitoring through onboard diagnostic systems.

- Periodic oil and filter changes (every 30, 000 km, ≈750 h, with modern synthetic lubricants).
- External component replacements (e.g., sensors, pumps, injectors).
- Fault detection and compensation through electronic on-board diagnosis (EOBD).
- No internal inspections or disassembly during the TBR.

This approach enables a low-maintenance and high-availability operational model. Maintenance tasks can typically be performed without engine removal and often directly onsite. Oil condition is monitored through capacitive dielectric sensors, and additional wear monitoring (e.g., magnetic chip detectors) can be integrated for aviation use.

Table 12 Maintenance philosophy comparison: automotive-derived diesel versus turboshaft engines

Aspect	Automotive diesel (aviation adaptation)	Turboshaft engines
Inspection method	EOBD diagnostics, no internal access	Borescope, teardown inspections
Routine maintenance	Oil/filter every 750 h, external parts only	Oil servicing + component tracking every few hundred hours
Overhaul cycle	Replacement-based (TBR: ∼4, 500 h)	Overhaul based (TBO: ∼3, 000–5,000 h)
Onsite maintainability	High (line-servicable)	Low (requires certified MRO facilities)
Monitoring tools	Capacitance oil sensors, optional chip detectors	Chip detectors + manual inspection protocols
Operational cost	Low (especially in off-design)	High (even at partial load)

It should be noted, however, that direct transfer of automotive maintenance philosophies to aviation applications is not straightforward. Aircraft propulsion systems are subject to significantly stricter safety, reliability, and certification requirements. Nevertheless, modern aircraft propulsion systems increasingly incorporate advanced diagnostic and health-monitoring technologies. Examples include full authority digital engine control (FADEC) systems and health and usage monitoring systems (HUMS), which are widely used in rotorcraft and turbine-powered aircraft to monitor engine condition, detect anomalies, and support predictive or condition-based maintenance strategies. These technologies demonstrate that software-based monitoring can play an important role in supplementing traditional inspection practices.

By contrast, traditional aerospace turboshaft engines operate under a much stricter and costlier maintenance regime. The typical TBO ranges from 2000 to 5000 h, but includes:

- Scheduled hot-section inspections (HSI), often halfway through TBO,
- Borescope inspections of turbine blades and combustion chambers,
- Mandatory teardown inspections for parts life tracking (e.g., turbine discs, bearings),
- Certified shop overhauls that require engine removal,
- Costly overhaul programs, often exceeding $300–500 per flight hour (fuel excluded).

In Table 12, the maintenance phases comparison between automotive-derived diesel engines and turboshaft engines is provided.

In this context, maintenance concepts inspired by automotive diesel practices may offer potential advantages in terms of operational cost and maintainability, particularly when combined with modern aircraft health monitoring technologies. Rather than replacing established aviation inspection procedures, such approaches could complement traditional maintenance strategies by enabling improved condition monitoring, earlier fault detection, and more efficient maintenance planning. The combination of software-based diagnostics, modular component replacement, and long service intervals may therefore contribute to reducing operational costs and downtime in certain applications, provided that reliability requirements and aviation certification standards are fully satisfied.

References

[1] Etele, J., and Rosen, M. A., 2001, "Sensitivity of Exergy Efficiencies of Aerospace Engines to Reference Environment Selection," Exergy, Inter. J., **1**(2), pp. 91–99.

[2] Dursun, O. O., Toraman, S., and Aygun, H., 2022, "Modeling of Performance and Thermodynamic Metrics of a Conceptual Turboprop Engine by Comparing Different Machine Learning Approaches," Inter. J. Energy Res., **46**(15), pp. 21084–21103.

[3] Nicolosi, F., Corcione, S., Trifari, V., and De Marco, A., 2021, "Design and Optimization of a Large Turboprop Aircraft," Aerospace, **8**(5), p. 132.

[4] Dinc, A., and Gharbia, Y., 2022, "Exergy Analysis of a Turboprop Engine at Different Flight Altitude and Speeds Using Novel Consideration," Inter. J. Turbo Jet-Eng, **39**(4), pp. 599–604.

[5] Ouyang, G., and An, S., 2019, *Common Rail Fuel Injection Technology in Diesel Engines*, Wiley, Hoboken, NJ.

[6] Xu, Y., 2024, "Revitalizing Diesel Technology in Aircraft: A Path Toward Fuel Efficiency and Sustainability," High. Sci., Eng. Technol., **119**, pp. 823–828.

[7] Zhao, W., Yan, J., Gao, S., Lee, T. H., and Li, X., 2022, "The Combustion and Emission Characteristics of a Common-Rail Diesel Engine Fueled With Diesel, Propanol, and Pentanol Blends Under Low Intake Pressures," Fuel, **307**, p. 121692.

[8] Altshuler, S. L., Ayala, A., and Collet, S., 2018, "Trends in On-Road Transportation, Energy, and Emissions," J. Air Waste. Manage. Assoc., **68**(10), pp. 1015–1024.

[9] Lloyd, A. C., and Cackette, T. A., 2001, "Diesel Engines: Environmental Impact and Control," J. Air Waste. Manage. Assoc., **51**(6), pp. 809–847.

[10] Topal, E., and Ramazan, S., 2010, "A New Mip Model for Mine Equipment Scheduling by Minimizing Maintenance Cost," Euro. J. Operat. Res., **207**(2), pp. 1065–1071.

[11] Piancastelli, L., and Frizziero, L., 2015, "Multistage Turbocharging Systems for High Altitude Flight With Common Rail Diesel Engines," J. Eng. Appl. Sci., **10**(1), pp. 370–375.

[12] Carlucci, A. P., Ficarella, A., Laforgia, D., and Renna, A., 2015, "Supercharging System Behavior for High Altitude Operation of an Aircraft 2-Stroke Diesel Engine," Energy. Convers. Manage., **101**, pp. 470–482.

[13] Szedlmayer, M., and Kweon, C. B., 2016, *SAE Technical Paper Series*, SAE International, Warrendale, PA.

[14] Yang, D., Cao, L., Liu, Y., and Zhang, Z., 2019, "Experimental and Numerical Investigation on a Novel Gas Turbocharging System for Diesel Engine Power Recovery at High Altitude," J. Mech. Sci. Technol., **33**(10), pp. 5061–5072.

[15] Jing, Q., Luo, Q., Gui, Y., and Liu, H., 2021, "Combustion Simulation of Variable Altitude Turbocharged Diesel Engine Using SVM," Inter. J. Auto. Technol., **22**(4), pp. 1087–1095.

[16] Gunston, B., 1989, *World Encyclopedia of Aero Engines*, 2nd ed., Patrick Stephens Ltd, Stroud, Gloucestershire, UK.

[17] Boito, M., Keating, E. G., Wallace, J., DeBlois, B., and Blum, I., 2015, "Metrics to Compare Aircraft Operating and Support Costs in the Department of Defense," RAND Corporation, Report No. RR-1178.

[18] Johnson, W., 2015, "Design and Analysis of Rotorcraft: Theoretical Basis and Architecture," NASA Report No. NASA TM-81182.

[19] Yüksel, B., Arslan, M., Aydemir, E., and Turan, O., 2025, "Comparative Performance Analysis of a Turboprop Engine Used in Regional Aircraft by Considering Design and Flight Conditions," Aircraft Eng. Aeros. Technol., **97**(3), pp. 345–359.

[20] AirNav LLC, 2025, "U.S. Jet-A Fuel Price Report: Average Retail Jet-A Prices at Fixed-Base Operators (FBOs)," AirNav LLC.

[21] International Air Transport Association (IATA), 2025, "Jet Fuel Price Monitor: Weekly Average Global Jet Fuel Price," IATA.

[22] U.S. Energy Information Administration (EIA), 2025, "Kerosene-Type Jet Fuel Spot Price, U.S. Gulf Coast (Dollars per Gallon)," U.S. Energy Information Administration (EIA), Database: Federal Reserve Economic Data (FRED).

[23] Pratt & Whitney Canada, 2013, "Service Bulletin No. 1703R9 – Engine Operating Time Between Overhauls and Hot Section Inspection Frequency," Pratt & Whitney Canada.

[24] Satpathy, N., and Murari, K., 2005, "Life Cycle Cost of a Six Ton Helicopter," J. Aeros. Sci. Technol., **57**(2), pp. 289–297.